ChemComm

Accepted Manuscript

This article can be cited before page numbers have been issued, to do this please use: Q. Zhang, X. Lu, H. Wang, X. Tian, A. Wang, H. Zhou, J. Wu and Y. Tian, *Chem. Commun.*, 2018, DOI: 10.1039/C8CC00908B.

View Article Online
DOI: 10.1039/C8CC00908B

Journal Name

COMMUNICATION

A benzoic acid terpyridine-based cyclometalated iridium (III) complex as two-photon fluorescence probe for imaging nuclear histidine under super resolution microscopy

Received 00th January 20xx,
Accepted 00th January 20xx

DOI: 10.1039/x0xx00000x
www.rsc.org/

Qiong Zhang[¶a], Xin Lu[¶a], Hui Wang[¶a,c], Xiaohe Tian[b*], Aidong Wang[d], Hongping Zhou[a], Jieying Wu[a]and Yupeng Tian[a,e*]

A series of two-photon active cyclometalated iridium (III) complexes (Ir1, Ir2 and Ir3) were designed. Ir1 with two-photon action cross-section of 40 GM in the NIR region has been developed for targeting intracellular histidine. Two-photon micrographs showed Ir1 could rapidly and selectively light up the nucleus in both fixed and live cells and capable of displaying nuclear histidine distribution with ultra details using super resolution (SR) technique under stimulated emission depletion (STED) microscopy.

Among the twenty amino acids, histidine is active in maintaining healthy tissues and protecting nerve cells that transport messages from brain to various the other parts of the body.[1-2] While in living cells, histidine acts as structural protein that closely associated with DNA and are known to manifest in a variety of ailments such as asthma and advanced liver cirrhosis.[3] Hence the development of high-quality methods for histidine detection is extremely necessary. Numerous studies have dealt with the detection of histidine using techniques such as voltammetry,[4] UV/vis spectroscopy,[5] luminescence spectroscopy methods [6] and fluorescence spectroscopy.[7] However, most of the available probes exhibit poor selectivity or require sophisticated detection systems such as the use of organic solvents. The development of reliable, rapid and accurate methods for the determination of histidine is still a highly challenging area. At present, visualization of intracellular histidine under two-photon microscopy (2PM) is an attractive approach. The advantages of two-photon excitation include reduced photobleaching, autofluorescence, non-invasive excitation, and deeper tissue penetration.[8-10] However, two-photon absorption (2PA) materials with moderate two-photon absorption cross-section (σ) values usually possess extended π-conjugated planar structures, consequently lead to biological unfriendly solvent (e.g. DMSO). Therefore, the design and synthesis of novel fluorescent probes with histidine specificity still remain challenge.[11]

[a]Department of Chemistry, Key Laboratory of Functional Inorganic Material Chemistry of Anhui Province, Anhui University, Hefei 230601, P. R. China
[b] School of Life Science, Anhui University, Hefei 230601, P.R. China
[c] Department of Chemistry, Wannan Medical College, Wuhu 241002, P.R. China
[d] School of Chemistry and Chemical Engineering, Huangshan University, Huangshan, P. R. China.
[e] State Key Laboratory of Coordination Chemistry, Nanjing University, Nanjing 210093, P. R. China
¶ These authors contributed equally to this work.
E-mail address:xiaohe.t@ahu.edu.cn; yptian@ahu.edu.cn.

Recently, the use of precious-metal complexes such as Ru(II), Ir(III), Pt(II)) as luminescent probes has attracted increasing interest due to their advantageous photophysical properties and low toxicity.[12] Among them, Cyclometalated iridium (III) complexes have gained increasing attention in the development of subcellular location agent or bio-probes due to their unique photophysical properties including large Stokes shifts and high photostability.[13]To date, iridium (III)-complex for detecting histidine (His) has been rarely reported.[14] And most of these cyclometalated iridium (III) complexes only have a tendency to be localized in mitochondria.[15] In this work, we reported a series of cyclometalated Iridium (III) complexes (Ir1-Ir3) for the purpose of nuclear histidine targeting. The considerations including its photon-physical properties and intracellular behaviours have been listed as follow: (1) Ir-C bond, constructed by 2-phenyl pyridine, was used to stabilize the energy levels of the Ir complexes. Subsequently, the two-photon absorption (2PA) activity was tuned by using terpyridine derivatives, owing to its strong electron-withdrawing ability, moderate π-conjugation system and strong binding affinity toward most metal ions.[11] (2) Compared to our previous work,[11, 16] new introduced carboxylic acid group can further influence the extent of electron delocalization and increase the solubility of the complexes, as well as good biocompatibility. Furthermore, carboxylic acid might accelerate the penetration of the Iridium (III) complex (**Ir1**) across the nuclear membrane as well as phenanthroline group with excellent planarity can connect with histidine. (3) The additional pyridine ring can provide a lone electron pair, which could be easily protonated and might lead to good water-solubility. For another, the pyridine ring possibly forms hydrogen bond with histidine to stable the molecule *in vivo* and *in vitro*.

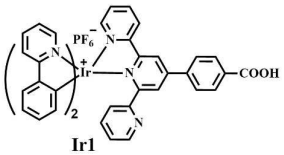

Ir1

*Scheme 1 The molecular structure of Ir(III) complex (**Ir1**).*

The synthesis procedures for **Ir1-Ir3** were outlined in Scheme S1. The crystal structural information reveals that the iridium (III) centre in **Ir2** adopts a distorted octahedral geometry (Scheme S1).One of the pyridine rings was not coordinated by **Ir1(III)** centre indicating that the extra free pyridine moiety is prone to target subcellular organelles.[11(a), 16] The linkage between the two planes was conjugated with the bond length is 1.439 Å (C00B-C00H) and 1.452 (C00S-C019) for **Ir2**, revealed that the bond length of C-C is located between the normal C=C double bond (1.32 Å) and C-C

View Article Online
DOI: 10.1039/C8CC00908B

single bond (1.53 Å). Notably, there is an active hydrogen atom being prone to dissociation and higher degree of electron delocalization in the carboxyl group (Fig S7), which arouse nonlinear optical response,[17] as well as may be sensitive to amino acids in living cells. The triplet Ir(III) complexes for use in two-photon processes require efficient intersystem crossing (ISC), large Stokes shifts and relatively long-lived triplet excited state lifetimes,[18,19] The band at 475 nm is assigned to a π^*(C-N) $\rightarrow\pi^*$(L) ligand-to-ligand charge-transfer (LLCT) transition, probably mixed with some ^{3}MLCT contribution (Fig S4(a)).The temperature-dependent shifts of the emission are typical of MLCT phosphorescence(Fig S4(b)), arising from different environments surrounding the molecule associated with stabilization of the polar MLCT emissive state. For supporting the experimental photophysical properties, TDDFT calculations showed the lowest-lying triplet state (T_1) is mainly described by the HOMO→LUMO excitation and has a ^{3}MLCT/^{3}LLCT nature. The second lowest state (T_2), which also has a ^{3}MLCT/^{3}LLCT nature, appears ~ 0.3 eV higher in energy than T_1 and presents some ^{3}LC character due to excitations centred on the ligand. These transitions are in keeping with the experimental results, which are contributed to two classes of transitions. (Fig S4(c) and Table S2).

The 2PA action cross-section (δ_{max}) of **Ir1** in DMSO/water (DMSO:H_2O = 1:9) was presented in Fig. S4(d), 1(c). The largest 2PA action cross-sections of Ir complexes were located around 780 ±20 nm with δ_{max} values between 20 - 40 GM. The intensities of 2PEF clearly exhibit the sequence of **Ir1** > **Ir3** >**Ir2**>**L**. Consistent with the above discussion, we found that a moderate extended-bridge can be reasonably increased the length of the conjugated chain and more favourable to electronic transitions floating, which is in agreement with the increase of the 2PA cross-section.

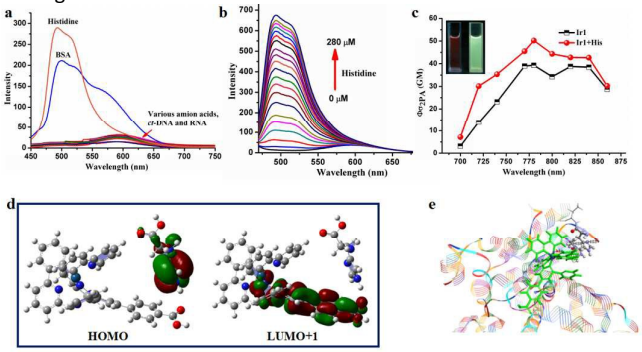

*Figure 1 (a) Emission spectra of **Ir1** (20 μM) with various amino acids[such as Ala, Arg, Asn, Gln, Glu, Gly, GSH, His, Ile, Leu, Lys, Met, Phe, Pro, Ser, Thr, Trp, Tyr, Val, Cys, Hcy], ct-DNA, RNA and BSA in PBS buffer (pH=7.4). (b) Changes in the luminescence emission spectra of **Ir1** (20 μM) with various amounts of histidine (0-14 equiv) in PBS buffer.(c) Two-photon action cross sections of **Ir1** in the presence or absence of His in PBS buffer(d)The frontier molecular orbitals distributions of **Ir1**-His. (e) Models obtained after molecular modeling of the interaction of **Ir1** with His.*

In order to evaluate their application *in vivo* and *in vitro*, **Ir1** was selected due to its largest 2PA cross-section (Fig. S4 (d)). **Ir1** exhibits a weak emission band at about 593 nm when excited at 405 nm. The interactions of **Ir1** with numerous intracellular substances including amino acids, proteins, DNA and RNA were examined by one and two-photon fluorescence experiments. Only histidine and BSA (histidine-rich protein) triggered a significant luminescence enhancement. Upon addition of increased concentrations of histidine (Fig 1(a,b)), a new emission at 493 nm was appeared and the intensity was increased corresponding to a blue shift of 100 nm. The phosphorescence intensity of **Ir1**at 493 nm (Φ < 1 %, τ=37.55 ns) was enhanced up 27-fold when the concentration of histidine was increased from 0 to 280 μM (Φ = 4.81 %, τ = 97.88 ns). The significant enhancement of the phosphorescence quantum yield suggests that **Ir1** is suitable for use in aqueous media. Besides that, the addition of peptides and proteins with different number of histidine residues induced enhancement in luminescence intensity of **Ir1**(Fig S8). The time plot of the emission intensity of **Ir1** interacts with (10 equiv) histidine was displayed in FigS9. The maximal phosphorescence signal of **Ir1** responding to histidine was reached within 10 min. In addition, the luminescence response of **Ir1** to proteins with a relatively high abundance of histidine residues, such as BSA, and 6 × histidine, was also investigated (Fig S10-S11). These results indicate that **Ir1** displays high selectivity for histidine/histidine-containing proteins *in vitro*. To explore the potential of **Ir1** for 2PFM applications, histidine induced obvious enhancement on 2PEF of **Ir1**, corresponding to that on one-photon excited fluorescence (1PEF) (Fig 11). In addition, the two-photon absorption action cross sections ($\Phi\sigma$) were further calculated to evaluate two-photon activity of **Ir1** and **Ir-His** (Fig 1(c), Fig S12). The $\Phi\sigma$ at 780 nm of **Ir1** increased from 40 GM to 48 GM (**Ir1-His**). This result indicates that **Ir1** has distinct changes in two-photon activity before and after reacting with His, which implies that **Ir1** is suitable for tracking histidine by using 2PFM technique.

To verify the above sensing mechanism, ^{1}H NMR titration experiments were carried out in d_6-DMSO:D_2O=9:1 (v/v). A significant peak split of hydroxy protons H_a and H_b was occurred after 2 equiv of histidine adding into **Ir1** solution, demonstrating the presence of secondary bonds interactions between carboxyl group of **Ir1** and imidazole group of histidine. The prominent peak at m/z 1009.2513 corresponding to the product [Ir1-His] was found using HRMS (Fig S13). The calculated frontier molecular orbitals and the calculated data of **Ir1** and **Ir1**-His were shown in Fig 1(d) and Table S3. For **Ir1**-His, the triplet excitations corresponding to the triplet-triplet transitions (498.5 nm) mainly originate from the HOMO→LUMO+1 transition. The distribution of LUMO+1 is similar to that of LUMO of **Ir1** and is mainly localized on the whole terpyridine ligand. However, the distribution of the HOMO of **Ir1**-His is significantly different from that of **Ir1,** which resides on the imidazole part of the histidine. Thus, an admixture of [$d\pi_{(Ir)}\rightarrow\pi^*_{terpyridine}$] ^{3}MLCT and ^{3}[$\pi_{imidazole}\rightarrow\pi^*_{terpyridine}$] ^{3}LLCT is responsible for the triplet-triplet transitions of **Ir1**-His, improving the emission of the iridium (III) complex. Therefore, the significant enhancement in emission intensity of **Ir1**-His may arise from a less nonradiative process and a favorable ICT process in the rigid molecular structure and the variation of transition characters. The mechanism was further confirmed *via* molecular modelling calculations using Discovery Studio Software.[20] The docking results (Fig. 1(f)) indicate that **Ir1** with suitable positive charge, lipophilicity which readily triggers histidine through secondary bonds interactions in different directions, which can stable with high Dock scoreand low CDOCKER energy.

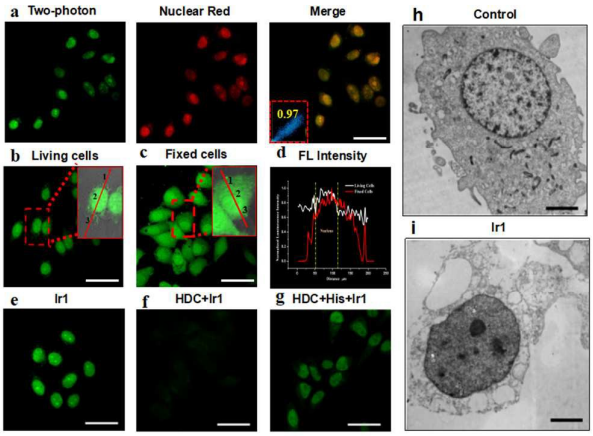

*Figure 2(a) Determination of intracellular localization of **Ir1** by confocal two-photon microscopy. HepG2 cells were incubated with Ir1 (10 μM, λ_{ex} = 820 nm, λ_{em} = 580-620 nm) for 10 min and then co-incubated with NucRed^{EM}(λ_{ex} = 638 nm, λ_{em} = 686 nm) for 10 min at 37 °C (inset: Pearson's coefficients Rr= 0.97), scale bar=20 μM. (b-(inset)) Amplified confocal two-photon*

View Article Online
DOI: 10.1039/C8CC00908B

fluorescence imaging of living HepG2 cells incubated with 10 μM ***Ir1****. (c-(inset)) Amplified confocal two-photon fluorescence imaging of fixed HepG2 cells incubated with 10 μM* ***Ir1.****(d) Two-photon fluorescence intensity profile across the line shown in corresponding to extracellular region (nucleus and cytoplasm). (e) Two-photon fluorescence images of* ***Ir1*** *in HepG2 cells: HepG2 cells incubated with* ***Ir1*** *(10 μM) for 30 min. (f) HepG2 cells pretreated with histidine decarboxylase (1.0 mM) for 30 min and then incubated with* ***Ir1*** *(10 μM) for 30 min. (g) HepG2 cells pretreated with histidine decarboxylase (1.0 mM) for 30 min and then incubated with histidine (400 μM) for 1 h, respectively, and finally incubated with* ***Ir1*** *(10 μM) for 1 h. (h)Cellular localization of* ***Ir1****characterized by transmission electron microscopy. TEM microscopy of HepG2 cells incubated with****Ir1****and stained without osmium tetroxide. (i) TEM microscopy of HepG2 cells incubated with complex* ***Ir1*** *stained without osmium tetroxide (right). (scale bar= 5 μm).*

To further explore their 2PM applications, MTT results of **Ir1** demonstrated that the relatively low toxic of the complex (Fig S14). The photostability of **Ir1** was shown that almost no obvious luminescence change was observed during ~250s continued irradiation (Fig S15). This indicated the high photostability of **Ir1** makes them favourable for long-term real-time tracking. We use HepG2 cells as a cell model incubated with **Ir1**, the colocolization experiments using commercially available nuclear stains Nuclear Red® (Fig2(a)) strongly suggested that **Ir1** targets cell nucleus in living cell with high signal-to-noise ratios (Fig 2(d)). Inductively coupled plasma (ICP)-MS was carried out to verify our speculation, the majority of iridium was localized and accumulated in the nucleus fraction of the cells which indicated "turn on" effect in nucleus (Fig. S16). Similar nuclear uptake was displayedapplying to other type of cancerous cells (Hela and A549)(Fig S17). Therefore, it was concluded that **Ir1** can selectively stain the nuclear region in varies cancer cells. Moreover, the specific nucleus staining by **Ir1** was achieved only for living cells and not for fixed cells. A generalized diffuse whole-cell staining pattern was observed by 2PM (Fig 2(b-c)) when HepG2 cells were fixed and further incubated with **Ir1.** Notably that normal cells HELF (Human Embryo Liver Fibroblast) displayed the diffusion of **Ir1**throughout cell cytosolic region and excluded from cell nucleus (Fig S18), this might suggestsnuclear uptake pattern of **Ir1** was cancerous specific, whereas its actual mechanism is still under investigation.

To further confirm the binding substance of **Ir1**in living cell nucleus is indeed histidine, histidine decarboxylase (HDC) that can be reacted with histidine specieswas used for pre-incubating with HepG2 cells. HepG2 cells showed luminescence off-on effect (Fig 2g) after histidine+**Ir1**treatment, strongly suggesting **Ir1** capable of targeting intracellular nuclear histidine with high specificity. Such confirmation was further proved by transmission electron microscopy experiment using **Ir1** due to its high electron density and intracellular *in situ* accumulation. Compared to control cells stained solely with osmium tetroxide (Fig. 2(h)), a phospholipid contrast reagent that has been widely used in electron microscopy, in the treated cells, subcellular membrane structures were clearly observed, including mitochondria, intracellular vesicles, plasma membrane and nuclear membrane.. It is found cell nuclear displayed much better contrast due to the binding of **Ir1** with nuclear histidine (Fig. 2(i)) while **Ir1** was used as solely contrast agent. These findings are again in agreement with the 2PM imaging, all strongly suggested that **Ir1**was located within nuclearin live cells with histidine specificity.

The cellular entry pathway of **Ir1** was also investigated as displayed in Fig S19. It shows that no luminescence was observed at 4°C, indicating that **Ir1** might enters cells through a temperature-dependent pathway. As **Ir1** has been successfully utilized as a convenient and noninvasiveness 2PA probe in living cells with superb photostability and cell permeability, it also showed good deep tissues penetration on a solid tumor model using HepG2 cells multi-cells spherical and displayed nuclear labeling. A significant fluorescence intensity was observed from the surface of spheroids to a depth of ~ 66 μm for **Ir1** (Fig S20), indicating a deep penetration of the two-photon excitation light.

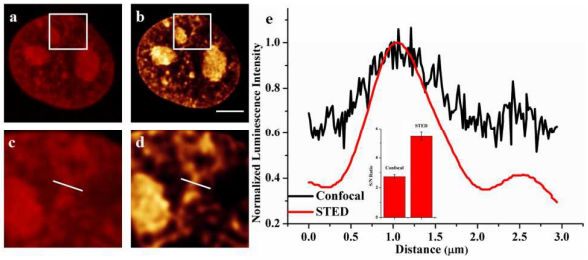

Figure 3 (a) Confocal two-photon fluorescence images of living HepG2 cells incubated with 10 μM ***Ir1*** *in DMSO/PBS (pH = 7.4, 1:99 v/v) for 10 min at 37 °C (λ_{ex} = 820 nm, λ_{em} = 580-620 nm). (b) The STED micrographs of Ir1 staining nucleolus in different numbers with higher resolution. (c-d) Amplified confocal two-photon fluorescence imaging and STED micrographsof living HepG2 cells incubated with 10 μM* ***Ir1****. (e) The fluorescence intensity profile shown in confocal two-photon fluorescence imaging and STED micrographs (inset: S/N ratio of confocal and STED).The scale bar= 5 μm.*

The successfulnuclear histidine labeling using **Ir1**demonstrated stable phosphorescence, high specificity, large Stock shift and long fluorescence lifetime (Table S1), we therefore further motivated to push its imaging utilization to display nuclear histidine in ultra-details under stimulated emission depletion (STED) microscopy in living cells. Initial studies carried out using TPM conditions, in which a 580-620 nm depletion beam was used, proved to be unsuccessful. Such observations indicate photoexcitation into a dark state. To address this issue, depletion using a 700 nm beam into the low-energy edge of the probe's broad emission was carried out. In this second set of conditions, STED images were successfully obtained, and using concentrations of **Ir1** as low as 10μM.Compare to normal confocal microscopy (Fig 3(a,c)), The STED micrographs clearly showed nuclear in higher resolution (Fig 3(b,d)) with much better signal-to-noise ratio(Fig 3(e)). The above results suggested that such cyclometalated iridium (III) complex**Ir1**can be used as a dual-model imaging probe under two-photon microscopy and STED microscopy for revealing intracellular Histidine. [21]

In summary, we designed and synthesized a series of novel Iridium (III) complexes (**Ir1~Ir3**) and investigated their photophysical properties in detail. **Ir1** has distinct changes in two-photon action cross section before and after reacting with Histidine from 40 to 48GM in NIR region. The *in vitro* binding assay, two-photon confocal microscopy and transmission electron microscopy elucidated that **Ir1** can be reacted with histidine/histidine-containing proteins to form a luminescent emissive product in living cancer cells'nuclear region through secondary bonds interactions. Further contribution using **Ir1** as an imaging tool in living cells under STEDnanoscopy successfully showed super resolution of nuclear, will provide many opportunities for the development of two-photon cyclometalated iridium (III) complexes for living cell-related studies.

This work was supported by the National Natural Science Foundation of China (21602003, 51672002, 21501001, 51432001 and 51472002), Postdoctoral Science Foundation of Anhui Province (2016B092), China Postdoctoral Science Foundation (2017M612050). Focus on returned overseas scholar of Ministry of Education of China, the Higher Education Revitalization Plan Talent Project (2013).

Notes and references

[1] G. N. Chen, X. P. Wu, J. P. Duan and H. Q, *Chen. Talanta.* 1999, 49, 319-330.

[2] T. E. Creighton, Encyclopedia of Molecular Biology. Wiley. New York.1999, vol. 2, p. 1147.

View Article Online
DOI: 10.1039/C8CC00908B

[3] D. J. SullivanJr, I. Y. Gluzman and D. E. Goldberg, Science, 1996, 271, 219-222.
[4]M. K. Amini, S. Shahrokhian and S. Tangestaninejad,*Anal. Chem.***1999**, 71, 2502-2505
[5] (a) S. Li, C. Yu and J. Xu, *Chem. Commun.***2005**, 450-452; (b) D. Xiong, M. Chen and H. Li, *Chem. Commun.* **2008**, 880-882.
[6] D. Ma, W. Wong, W. Chung, F. Chan, P. So, T. Lai, Z. Zhou, Y. Leung and K. Wong, *Angew. Chem. Int. Ed.* **2008**, 47, 3795-3799.
[7] (a) M. Kruppa, C. Mandl, S. Miltschitzky and B. Konig, *J. Am. Chem. Soc.***2005**, 127, 3362-3365; (b) F. Pu, Z. Huang, J. Ren and X. Qu, Anal, *Chem.Commun,* **2011**, 47, 3487-3489.
[8] (a) D. Chen, Y. Pan, L. Wang, Z. B. Zeng, L. Yuan, X. B. Zhang and Y. T. Chang, *J. Am. Chem. Soc.*, **2017**, 139(1), 285-292.(b) W. B. Hu, M. Xie, H. Zhao, Y. F. Tang, S. Yao, T. C. He, C. X. Ye, Q. Wang, X. M. Lu, W. Huang and Q. L. Fan, *Chem. Sci.* **2018,** 9, 999-1005
[9] (a) W. Du, H. Wang, Y. Z. Zhu, X. H. Tian, M. Z. Zhang, Q. Zhang, S. C. D. Souza, A. D. Wang, H. P. Zhou, Z. P. Zhang, J. Y. Wu and Y. P. Tian, *ACS Appl. Mater. Interfaces.*, **2017**, 9(37), 31424-31432. (b) J. G. Jia, Y. Zhang, M. Zheng, C. F. Shan, H. C. Yan, W. Y. Wu, X. Gao, B. Cheng, W. S. Liu and Y. Tang, *Inorg. Chem*. **2018**, 57, 300-310.
[10] (a) H. M. Kim and B. R. Cho,*Chem. Rev.***2015**, 115(11), 5014-5055;(b) K. A. Chan and S. G. Kazarian, *Chem. Soc. Rev.* **2016**, 45(7), 1850-1864. (c)G. Xu, S. Zeng, B. Zhang, M. T. Swihart, K. T. Yong and P. N. Prasad, *Chem. Rev.***2016**, 116(19), 12234-12327.
[11] (a) X. H. Tian, Y. Z. Zhu, M. Z. Zhang, L. Luo, J. Y. Wu, H. P. Zhou, L. J. Guan, G. Battaglia and Y. P. Tian, *Chem.Comm.,* **2017**, 53, 3303-3306.(b) X. H. Tian, Q. Zhang, M. Z. Zhang, K. Uvdal, Q. Wang, J. Y. Chen, W. Du, B. Huang, J. Y. Wu and Y. P. Tian, *Chem. Sci.*, **2017**, 8, 142-149.
[12] (a) H. K. Saeed, P. J. Jarman, S. Archer, S. Sreedharan, I. Q. Saeed, L. K. Mckenzie, J. A. Weinstein, N. J. Buurma, C. G. W. Smythe and J. A. Thomas, *Angew. Chem.* **2017**, 129, 12802-12807. (b) Y. Chen, T. W. Rees, L. N. Ji and H. Chao, Current Opinion in Chemical Biology, **2018**, 43, 51-57
[13] (a) C. Yang, F. Mehmood, L. T. Lam, F. L. S. Chan, Y. Wu, S. C. Yeung, G. X. Guan, K. Li, S. Y. C. Chung, Y. C. Zhou, T. T. Zou, M. C. Che, *Chem. Sci.***2016**, *7*, 3123-3136. (b) K. P. S. Zanoni, A. Ito, M. Grüner, N. Y. M. Iha and A. S. S. de Camargo, *Dalton Trans*. **2018,** 47, 1179-1188
[14] C. Y. Li, M. X. Yu, Y. Sun, Y. Q. Wu, C. H. Huang and F. Y. Li, *J. Am. Chem. Soc.***2011**, 133, 11231-11239.
[15] C. Yang, F. Mehmood, T. L. Lam, S. L. F. Chan, Y. Wu, C. S. Yeung, X. G. Guan, K. Li, C. Y. S. Chung, C. Y. Zhou, T. T. Zou, C. M. Che, *Chem. Sci.***2016**, *7*, 3123-3136.
[16] H. Wang, L. Hu, W. Du, X. H. Tian, Z. J. Hu, Q. Zhang, H. P. Zhou, J. Y. Wu, K. Uvdal and Y. P. Tian, *Sensors and Actuators B.***2018**, 255, 408-415.
[17] G. Calogero. G. Giuffrida, S, Serroni, V. Ricevuto. S. Campagna, Absorption Spectra, *Inorg. Chem*. **1995**, 34, 541−545.
[18] D. M. Li, X. H. Tian, G. J. Hu, Q. Zhang, P. Wang, P. P. Sun, H. P. Zhou, X. M. Meng, J. X. Yang, J. Y. Wu, B. K. Jin, S. Y. Zhang, X. T. Tao and Y. P. Tian, *Inorg. Chem.***2011**, 50, 7997-8006.
[19] (a) X. H. Tian, Y. Z. Zhu, M. Z. Zhang, L. Luo, J. Y. Wu, H. P. Zhou, L. J. Guan, G. Battaglia and Y. P. Tian, *Chem.Comm.*.**2017**, 53, 3303-3306.(b) K. Y. Zhang, K. K. W. Lo, Inorg. *Inorganic chemistry*.**2009**, 48, 6011-6025.
[20] C. M. Venkatachalam, X. Jiang, T. Oldfield, M. Waldman, *J. Mol. Graph. Model.* **2003**, 21, 289-307.
[21] (a) S. Sreedharan, M. R. Gill, E. Garcia, H. K. Saeed, D. Robinson, A. Byrne, A. Cadby, T. E. Keyes, C. Smythe, P. Pellett, J. B. de la Serna and J. A. Thomas, *J. Am. Chem. Soc.*, **2017**, 139(44), 15907-15913. (b) A. Byrne, C. S. Burke and T. E. Keyes, *Chem. Sci.*, **2016**, 7, 6551-6562. (c) A. Byrne, C. S. Burke, T. E. Keyes, Chem. Sci., 2016, 7, 6551-6562